OPEN ACCESS

University of BRISTOL

Luo, J., Jiang, J. Z., & Macdonald, J. (2016). Damping Performance of Taut Cables with Passive Absorbers Incorporating Inerters. In 13th International Conference on Motion and Vibration Control (MOVIC 2016) and the 12th International Conference on Recent Advances in Structural Dynamics (RASD 2016): 4–6 July 2016, Southampton, UK. [012046] (Journal of Physics: Conference Series; Vol. 744, No. 1). IOP Publishing. DOI: 10.1088/1742-6596/744/1/012046

Publisher's PDF, also known as Version of record

License (if available):
CC BY

Link to published version (if available):
10.1088/1742-6596/744/1/012046

Link to publication record in Explore Bristol Research
PDF-document

University of Bristol - Explore Bristol Research
General rights

Damping Performance of Taut Cables with Passive Absorbers Incorporating Inerters

You may also be interested in:

Damping Performance of Taut Cables with Passive Absorbers Incorporating Inerters

Jiannan Luo, Jason Zheng Jiang and John H G Macdonald
Faculty of Engineering, University of Bristol.

Abstract. As stay cables are prone to vibrations due to their low inherent damping, a common method to limit unwanted vibrations is to install a viscous damper normal to the cable near one of its supports. This paper investigates the potential performance improvement that can be delivered by a numbers of candidate absorbers that incorporate inerters. The inerter device is the true network dual of a spring, with the property that the force is proportional to the relative acceleration between its two terminals. A finite element taut cable model is used for this study. A specific cost function indicating the damping performance of a cable with an absorber attached is proposed. An optimisation of the performance is then carried out. Based on optimisation results, the best damping performance for each of the candidate absorber structures against a specific range of inertance values is presented.

Keywords. Stay cable, passive absorber, inerter, vibration suppression

1. Introduction
Stay cables are widely used in cable stayed bridges and other civil engineering structures in order to carry static loads. It is important for cables to ensure the safety of the entire structure [1]. However, resonance of cables will cause large amplitude vibrations due to their low inherent damping. Typically, the inherent damping ratio of cables on suspension bridges is about 0.1% [2]. So, unless suppressed, either direct load on cables from environment or minor motion at the cable supporting ends will cause vibrations [3]. But, only modes with low natural frequency, typically the first six modes of the cable are being considered as they typically experience more severe vibrations than high natural frequency modes [4].

Several studies have been made in order to understand the dynamic behaviour of taut cables and their vibration behaver using viscous damper. Irvine and Caughey [5] developed a linear theory for the free vibration of uniform suspended cable. Yoneda & Maeda [6] proposed the use of a set of empirical equations for defining the optimum damper size. Later, Pacheco et al. [1] determined the universal curve for estimating the modal damping of stay cables and Krenk [7] gave an analytical formula for the universal curve, based on complex modes analysis. More recently, Main and Jones [8] extended these studies to the case when the presence of linear viscous dampers induces large shifts of the cable natural frequency.

In order to limit unwanted vibrations on cables, viscous dampers and tuned mass dampers (TMDs) have been used in practice. For both structures, the optimum damping ratio for a certain mode is larger if the damper located closer to the antinode of that mode [6]. Viscous dampers are normally installed normal to the cable, for ease of manufacture and maintenance, they should be located close to the supporting end to the deck, usually less than 5% of the way alone the cable [4]. However, being close to the cable end, a viscous damper may not be effective enough for vibration suppression of multiple modes. The TMD structure is more effective and it can be located at any position along the cable. However, it needs

a relatively heavy secondary mass to be beneficial for multiple modes, and for maintenance it is undesirable for it to be too high on the cable [10].

This paper investigates the performance of several inerter combined vibration absorbers. The inerter was proposed as an ideal two terminal mechanical element, in which the applied force is proportional to the relative acceleration between its two terminals. By using the force-current analogy, mechanical circuits can be translated to classical electrical circuits in a completely analogous way [11]. Research has been carried out to introduce this new device into traditional vibration suppression systems. Recent results show that inerter combined structures can effectively improve the performance of vehicle suspensions [12], motorcycle suspensions [13], train suspensions [14][15], and building structures [16][17]. For vibration suppression on cables, a methodology has proposed to obtain the optimum damping ratio for a tuned inerter damper (TID) system [18].

The aim of this paper is to systematically study the optimum critical damping ratios that can be achieved by absorber structures incorporating inerters, which is organised as follows. Firstly, a finite element model of the cable is built in order to study the behaviour of the cable with different absorber structures. Then, the performance of a viscous damper and three other candidate absorber structures incorporating inerters has been studied. Finally, based on the optimisation results, the damping performance of each configuration are compared and assessed accordingly.

2. Mathematical Approach
In this section, a finite element cable model is introduced firstly. Then, four candidate absorber structures and the optimisation criterion for damping performance are discussed.

2.1. Mathematical model of a cable including an absorber
The mathematical model of the cable is modelled by the finite element algorithm, which is considered as a system modelled with lump mass elements with negligible flexural stiffness. The tension force alone the cable is denoted as T, the total mass of the cable is M, the total span length of the cable is L. The effect of inclination and sag of the cable are neglected as well as cable's out-of-plane motion and elasticity. For a cable with n degrees of freedom (DOF), there are all together $n + 2$ masses, n masses m, are spread alone the cable, two masses, $m/2$, are connected directly to the supporting ends. Hence, $m = M/(n + 1)$. The masses divide the cable into $n + 1$ lengths $l = L/(n + 1)$. The ath mass has an associated vertical position $x_a(t)$ simplified as x_a, which is zero at equilibrium. Since the end masses are connected directly to the supports, x_0 and x_{n+1} are considered identically equal to zero. An example of a taut cable model with five DOF is shown in Figure 1.
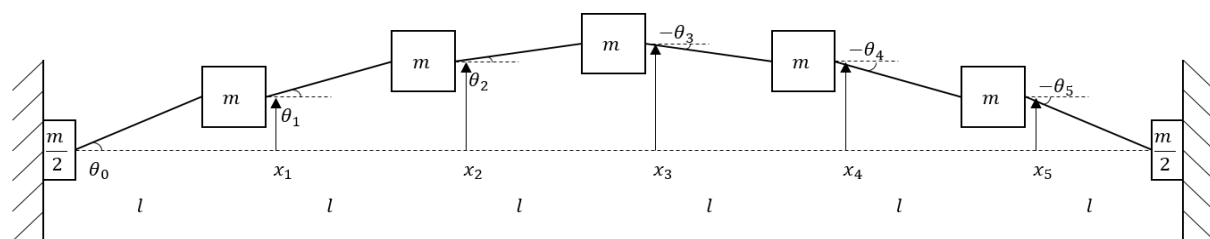
Figure 1. Finite element simulation model of a taut cable (with five DOF)

For a vibrating cable model with n DOF, the displacement of the masses from their vertical equilibrium positions lead to an angle θ_a between mass $a + 1$ and mass a. As vertical displacements are relatively small compared to the element length $L/(n + 1)$, the angle θ_a can be presented by

$$\theta_a = \arcsin(\frac{x_{a+1} - x_a}{L/(n+1)}) . \tag{1}$$

The equation of motion for mass a without any external force can be expressed as

$$m\ddot{x}_a = T\sin(\theta_a) - T\sin(\theta_{a-1}) . \tag{2}$$

According to Mersenne's laws, the fundamental frequency of the undamped cable can be calculated as $f_o = 0.5L \cdot (T/u)^{0.5}$, where u is the mass per unit length. Therefore, the natural circular frequency of mode 1 of the undamped cable is can be expressed as

$$\omega_o = \pi \cdot (T/ML)^{0.5} \tag{3}$$

By substituting Equation (1) and (3) into (2), Equation (4) can be obtained.

$$\frac{1}{n+1}\ddot{x}_{a_f} = (n+1) \cdot \left(\frac{\omega_o}{\pi}\right)^2 \cdot \left(x_{a_f+1} - 2x_{a_f} + x_{a_f-1}\right) . \tag{4}$$

Similarly, the equation of motion for mass a_f of a cable is expressed as Equation (5), at which an external force $F(t)$ is provided by an absorber.

$$m\ddot{x}_a = T\sin(\theta_a) - T\sin(\theta_{a-1}) + F(t) . \tag{5}$$

By substituting Equation (1) and (3) into (5), Equation (6) can be obtained.

$$\frac{1}{n+1}\ddot{x}_{a_f} = (n+1) \cdot \left(\frac{\omega_o}{\pi}\right)^2 \cdot \left(x_{a_f-1} - 2x_{a_f} + x_{a_f+1}\right) + \frac{F(t)}{M} . \tag{6}$$

By rearranging the vertical position, speed and acceleration of each mass unit into vectors in the format of $x = [x_1, x_2, x_3, \ldots, x_n]^T$, Equations (4) and (6) can be rearranged into matrix format with matrices $\mathbf{M}$, $\mathbf{C}$ and $\mathbf{K}$, i.e.

$$\mathbf{M}\ddot{x} + \mathbf{C}\dot{x} + \mathbf{K}x = \mathbf{0} . \tag{7}$$

By taking Laplace transformation for both sides, Equation (7) can be expressed as (8)

$$\mathbf{M}s^2\tilde{x} + \mathbf{C}s\tilde{x} + \mathbf{K}\tilde{x} = \mathbf{0} . \tag{8}$$

In Equation (8), matrices $\mathbf{M}$, $\mathbf{C}$ and $\mathbf{K}$ are respectively represented by Equations (9)-(11), in which δ_{ij} is the Kronecker delta function. $Y(s)$ represents the admittance function of the absorber. The admittance in mechanical is define to be the ratio of the force to velocity, which agrees with the usual electrical terminology [11]. In this study, $Y(s) = \tilde{F}(s)/[s \cdot \tilde{x}_{a_f}(s)]$, assuming that one end of the absorber connected to mass a, while the other end of the absorber is attached to a fixed support.

$$\mathbf{M}_{ij} = \frac{1}{n+1}\delta_{ij} , \tag{9}$$

$$\mathbf{C}_{ij} = 0, \text{ except } \mathbf{C}_{a_f a_f} = -Y(s) , \tag{10}$$

$$\mathbf{K}_{ij} = (n+1) \cdot \left(\frac{\omega_o}{\pi}\right)^2 \cdot \left(2\,\delta_{ij} - \delta_{i(j+1)} - \delta_{i(j-1)}\right) . \tag{11}$$

With matrices $\mathbf{M}$, $\mathbf{C}$ and $\mathbf{K}$ as input, a set of complex eigenvalues of the system can be calculated via Equation (12), where $\boldsymbol{\lambda} = [\lambda_1, \lambda_2, \lambda_3, \ldots, \lambda_n]$, $\mathbf{0}$ is a square null matrix of size n, $\mathbf{I}$ is a unit matrix of size n.

$$[\boldsymbol{\lambda} \quad \boldsymbol{\lambda}^{*T}]^T = \text{eig}\begin{bmatrix} \mathbf{0} & \mathbf{I} \\ -\mathbf{M}^{-1}\mathbf{K} & -\mathbf{M}^{-1}\mathbf{C} \end{bmatrix} . \tag{12}$$

$[\boldsymbol{\lambda} \quad \boldsymbol{\lambda}^{*T}]^T$ is a vector of size $2n$, which provides a set of complex eigenvalues which are in n complex conjugate pairs. Either eigenvalue λ_e or its complex conjugate eigenvalue λ_e^* can be used to calculating damping ratio ζ_e and natural frequency ω_e of mode e of the damped cable, respectively expressed by Equations (13) and (14).

$$\zeta_e = |\text{Re}(\lambda_e)/\text{Im}(\lambda_e)| , \tag{13}$$

$$\omega_e = |\text{Im}(\lambda_e)| . \tag{14}$$

In principle, in order to reduce the error due to finite-series approximation, the number of DOF n should be as large as possible. However, in order to limit the computational time, n is selected to be 19 for this study.

2.2. Candidate absorber structures and optimisation criterion

The four candidate absorber structures are shown in Figure 2, where one terminal of the structure is connected to the cable at mass a_f and the other is attached to a fixed support. Structure I represents a traditional viscous damper. Structure II and III comprise a damper and inerter in parallel and in series respectively. Structure IV is the same as the TID structure introduced in reference [18], which is similar to the TMD structure except that the inerter is applied rather a mass unit.
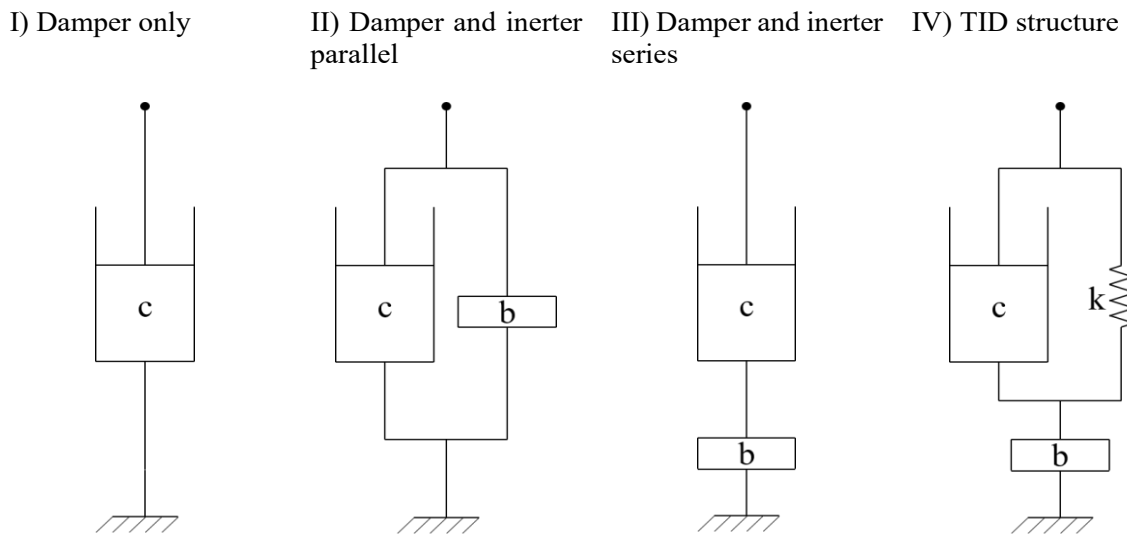

I) Damper only   II) Damper and inerter   III) Damper and inerter   IV) TID structure
                          parallel   series

Figure 2. Structure of four candidate absorbers

For a taut cable with an attached absorber, if vibration energy can be effectively transferred and dissipated, the cable vibration will be effectively reduced. Therefore, damping ratio ζ is selected to be the key parameter to judge the effectiveness of the absorber. Here, the elements in the four candidate absorbers are considered to be ideal, so the admittance function of the absorber $Y(s)$ contains the parameters of damping coefficient c, inertance b and stiffness k.

For simplicity, the parameters of the system are presented in non-dimensional form as $c' = (c/M)/\omega_0$, $b' = b/M$ and $k' = (k/M)/\omega_0{}^2$. Similarly, the damped natural frequency ω and the location of the absorber a_f are also presented in non-dimensional form as $\omega' = \omega/\omega_o$ and $a_f' = a_f/n$. The admittance function of the four candidate absorbers are $Y_1(s) = c$, $Y_2(s) = bs + c$, $Y_3(s) = 1/(\frac{1}{c} + \frac{1}{bs})$, $Y_4(s) = 1/(\frac{1}{c+k/s} + \frac{1}{bs})$, repectively.

Previous studies show that structure I and Structure IV are more efficient for a particular mode if they are located close to the anti-node point of that mode [4][7]. The location of the absorber relative to the total length of the cable, which presented as a_f' should be large enough for optimising the damping ratio for low natural frequency modes. However, for all four candidates, in reality $a_f' = 5\%$ should be the maximum ratio due to installation and maintenance problem. Therefore, to be comparable, the location a_f' is set to be 5% for all four candidate absorber structures presented in this study.

If sag and other minor effects are neglected, the vibration mode with the lowest natural frequency will be the most severe case among all modes. However, in some cases, adding absorbers may lead to significant changes of natural frequency or extra modes being introduced. These may cause the natural frequencies of some modes to be close to or even lower than the natural frequency of origin undamped mode 1. In this study, a frequency range of $0 \sim 1.5\omega_o$ is selected in order to cover the damped natural frequency of mode 1 and other low natural frequency modes caused by the factors mentioned above.

For optimisation, the effectiveness of the absorber is judged by the critical damping ratio ζ_c, which is defined as the lowest damping ratio among all modes with natural frequencies in the range of $0 \sim 1.5\omega_o$. The optimum critical damping ratio for the cable with each structure is calculated via a Matlab script using the non-linear optimisation algorithm called 'fminsearch' [19].

For Structure I, the non-dimensional damping coefficient c' is searched for the c' value which provides the optimum critical damping ratio ζ_c. This result is compared with previous research and taken as a reference with which to compare with other structures. For Structures II, III and IV, inerters with b' ranged from 0 to 2.5 are used for optimisation. For each given b', rest parameter values in the structures are searched to optimize the critical damping ratio ζ_c. The mode(s) which contain the all critical damping ratios is defined as the critical damping mode.

3. Optimum performance for candidate absorber structures

In this section, the optimum critical damping ratios for all four candidate structures are calculated and compared accordingly. Figures are drawn to show the optimum critical damping ratios ζ and their corresponding non-dimensional natural frequencies ω'.

3.1. Optimum results for Structure I

A viscous damper, i.e. Structure I, is a suitable structure to supress cable vibrations, which has been thoroughly studied. Several researchers have provided different methods in order to understand the resulting dynamic behaviour for a viscous damper attached to a cable. Their results provide the relationship between the damping ratio ζ and the system parameters namely the non-dimensional damping coefficient c', the relative location of the absorber a_f' and the mode number e. According to their research, the optimum damping ratio for each mode of the cable is approximately $\zeta = 0.5 \cdot a_f'$, which shows that the optimum performance of viscous dampers is limited by their location relative to the support.

According to the optimisation approach introduced in Section 2, the modes with natural frequencies in the range $0 \sim 1.5\omega_o$ are considered. As shown in Figure 3(b) only one mode is inside that frequency range for a cable with Structure I. The optimum critical damping ratio ζ_c provided by the viscous damper corresponding to a natural frequency in the range is $\zeta_c = 0.0264$ when $c' = 6.441$, as shown in Figure 3(a). This is consistent with the result of previous studies [1][7].
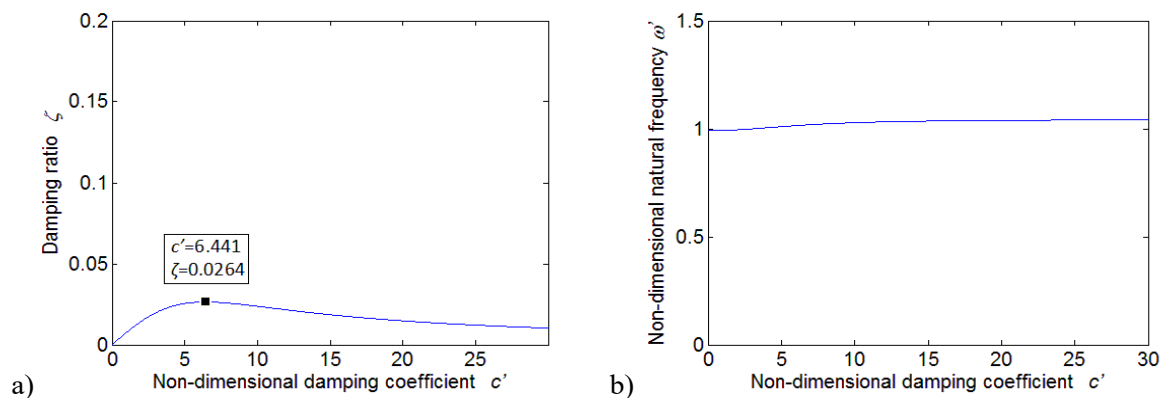

Figure 3. Results for Structure I with varying c' for $a_f' = 0.05$. (a) Damping ratio versus damping coefficient of the damper. (b) Corresponding non-dimensional natural frequency.

3.2. Optimum results for Structure II

The optimum results for a range of values of the non-dimensional inertance b' for cable with Structure II are shown in Figure 4. For $b' = 0$, the solution is the same as the optimum solution in Figure 3. It can

be seen that for $b' > 0$, Structure II can provide better optimum critical damping ratio ζ_c than that of a viscous damper for any inertance b' used in the present simulation cases.

In Figure 4(a), the blue solid curve indicates the critical mode, which is composed of the optimised critical damping ratios ζ_c for each given inertance b'. The green dashed curve shows the solution for a simultaneously-occurring mode with a natural frequency in the range of $0 \sim 1.5\omega_o$ which is non-critical. The corresponding frequencies of both modes are shown in Figure 4(b). The line styles are consistent for Figure (5-7) with those used in Figure 4.
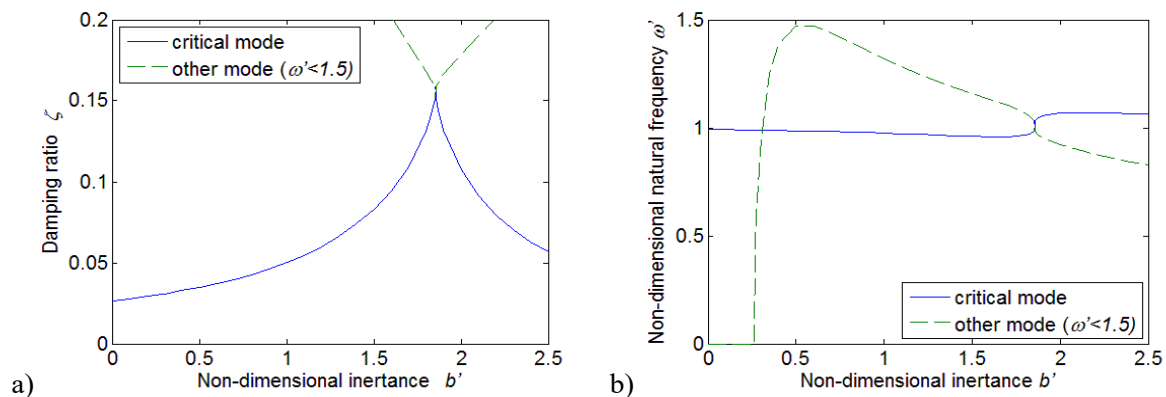

Figure 4. Optimisation results for Structure II with varying b' for $a_f' = 0.05$. (a) Damping ratio versus non-dimensional inertance of the damper. (b) Corresponding non-dimensional natural frequency.

It can be seen from the blue solid curve in Figure 4(a) that among all the optimised results with varying b', Structure II can provide maximum optimum critical damping ratio of $\zeta_c = 0.156$ for $b' = 1.855$. This is 5.9 times of that from a viscous damper only (Figure 3(a)). It can be seen in Figure 4(b) that the natural frequency of the critical mode is similar to that of the original undamped mode 1. At $b' = 1.855$ the solutions for the critical and the non-critical modes cross over each other, which leads to the breakpoint in Figure 4(a).

3.3. Optimum results for Structure III
Figure 5 shows the optimum result for Structure III for a range of values of the non-dimensional inertance. It can be seen that the result are at a similar from to those for Structure II. Structure III is hence another beneficial structure compared with a viscous damper only if non-dimensional inertance b' is large enough. It can be seen in Figure 5(a) that among all the optimised results with varying b', the absorber of Structure III can provide maximum optimum critical damping ratio of $\zeta_c = 0.160$, for $b' = 2.363$. This is 6.1 times of that provided by a viscous damper, and it is slightly better than result provided by Structure II shown in Figure 4(a). However, Structure III has drawback that a relatively large b' is needed for optimum ζ_c to be large. The optimum ζ_c of Structure III is larger than that of a damper alone, only if $b' > 1.15$.
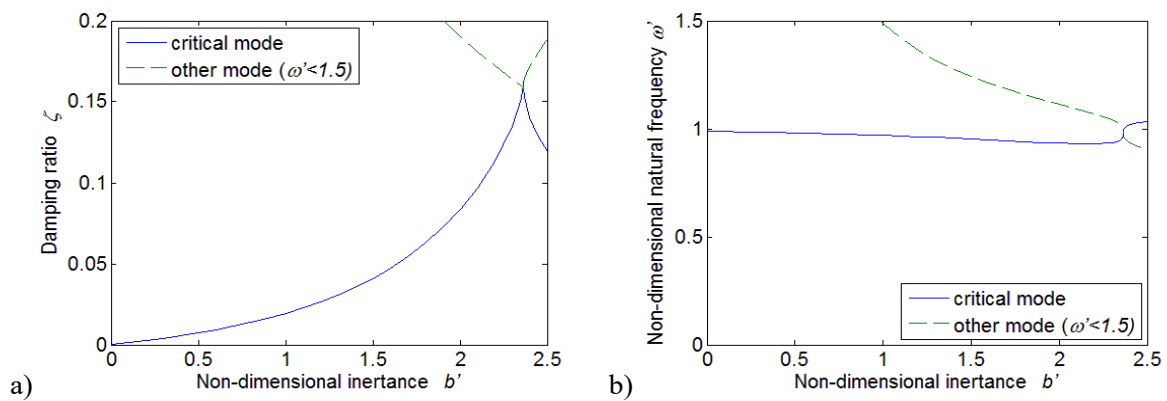
Figure 5. Optimisation results for Structure III with varying b' for $a_f' = 0.05$. (a) Damping ratio versus non-dimensional inertance of the damper. (b) Corresponding non-dimensional natural frequency.

Similar to the case for Structure II, it can be seen in Figure 5(b) that the natural frequency of the critical mode are close to that of the original undamped mode 1. The breakpoint at $b' = 2.363$ in Figure 5(a) can be observed due to the crossover of the two modes.

3.4. Optimum results for Structure IV
It can be seen in Figure 6(a) that among all the optimum results with varying b', the absorber of structure IV can provide maximum optimum critical damping ratio of $\zeta_c = 0.160$, for $b' = 2.363$. Compared with Structure III, Structure IV has the same maximum optimum ζ_c as Structure III, but Structure IV is more effective when b' is relatively small.
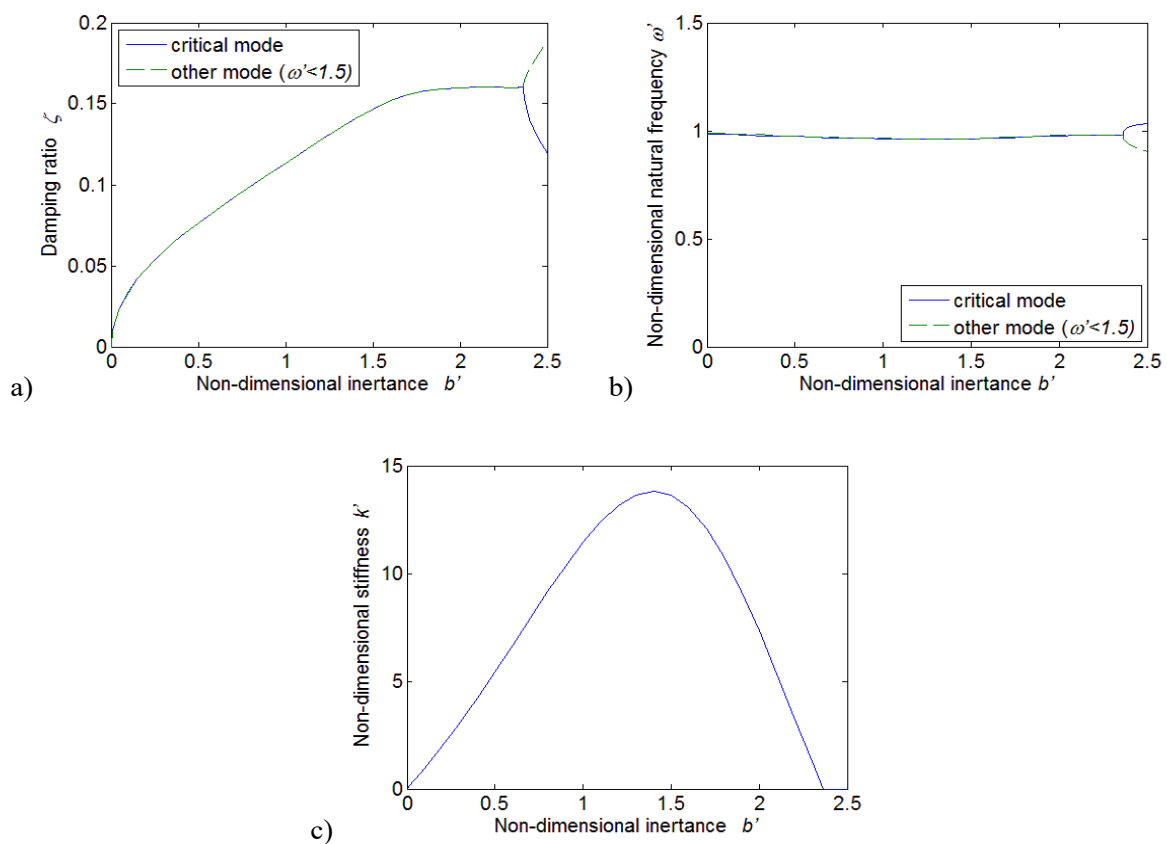
Figure 6. Optimisation results for Structure IV with varying b' for $a_f' = 0.05$. (a) Damping ratio versus non-dimensional inertance of the damper. (b) Corresponding non-dimensional natural frequency. (c) Corresponding non-dimensional stiffness.

For any optimised ζ_c with a given inertance $b' \leq 2.363$. The two modes of the system with $\omega' < 1.5$ provide the same damping ratio and vary similar natural frequencies (Figure 6(b), approximately 0.1% different). When $b > 2.363$, the two modes bifurcate. This is because the non-dimensional stiffness k' for the optimum has reduced to zero (Figure 6(c)). Since k' cannot physically be negative, for $b > 2.363$ the optimum value of k' is zero and the solution are then the same as for Structure III.

3.5. Comparison of all four structures
Figure 7 shows the optimum critical damping ratio with mass ratio b' ranged from 0 to 2.5 for all four structures. For Structure I, since b' always equal to zero, the optimum critical damping ratio is marked as a cross on Figure 7. It can be seen that, all other three structures comprising one inerter can be more beneficial with suitable b'. The optimum critical damping ratio of Structure I is $\zeta = 0.0264$. For Structure II, the maximum optimum critical damping ratio with varying b' is $\zeta = 0.156$ with $b' = 2.363$. For Structure III and Structure IV (TID), the maximum optimum critical damping ratios are the same, which is $\zeta = 0.160$ with $b' = 2.363$. When $b' > 2.363$, optimum critical damping ratios for Structure III and IV are the same. This is due to the fact that the optimum non-dimensional stiffness $k' = 0$ for Structure IV with $b' = 2.363$.
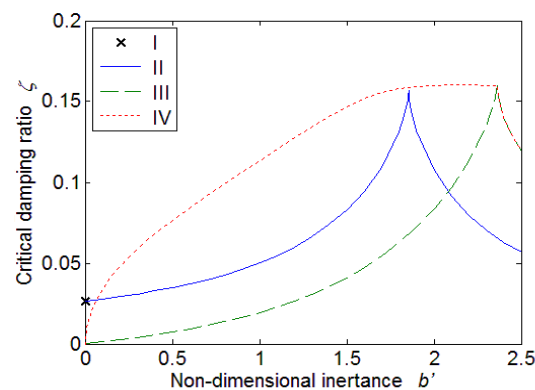

Figure 7. Comparison of optimum ζ with varying b' for all four structures ($a_f' = 0.05$) with varying b', ranged from 0~2.5.

Based on Figure 7, it can be concluded that all three structures with inerters are far more beneficial than damper with suitable b' is. Within the vibration structures considered, the most beneficial structure for b' within the range (0, 0.07], (0.07, 2.363] and (2.363, 2.5], are Structure II, Structure IV and Structure III & IV, respectively. Even though the Structure IV is the most effective structure for a large range of b values, it should be noted that a device with large inertance is hard to be manufactured. For this reason, the benefit provide by Structure II cannot be neglected.

4. Conclusions
In this paper, a FE model of the cable is introduced. The damping performance of three vibration absorber structures of cables were analysed and compared with a traditional viscous damper. The concept of critical damping ratio was proposed and used as the performance criterion for optimisation. Based on the results, all three structures can provide improvement over traditional damper with suitable inertance values. The conclusion of the optimum structures with respect to the non-dimensional inertance viable b' within the range (0, 2.5) were presented.

The results shows that all three structures with inerters can provide better optimum damping ratio compared with structure I, viscous damper connected at the same location with suitable range of inertance b' selected. Furthermore, in a relatively broad range of b' (0.07, 2.5], Structure IV (TID) is the most beneficial structure among the all structures studied.

Reference
[1]   Pacheco B M, Fujino Y and Sulek A, 1993. Estimation curve for modal damping in stay cables with viscous damping. Journal of Structural Engineering, **119**(6), 1961-1979.
[2]   Yamaguchi H, Fujino Y, 1998. Stayed cable dynamics and its vibration control. Proceedings International Symposium on Advances in Bridge Aerodynamics, Balkema, Rotterdam, Netherlands, 235–253.
[3]   Waston S C and Stafford D, 1998. Cables in trouble. Civil Engineering, ASCE, **58**(4), 38-41.
[4]   Gimsing N J, 2012 & Georgakis C T. Cable Supported Bridges: Concept and Design, 3nd edition. Wiley.
[5]   Irvine H M and Caughey T K,1974. The linear theory of free vibration of a suspended cable. Proc. of the royal soc of London, series A, **341**: 299-315.
[6]   Yoneda M and Maeda K, 1989. A study on practical estimation method for structural damping of stay cable with damper, Proceedings of Canada-Japan Workshop on Bridge Aerodynamics, Canada, 119-128.
[7]   Krenk S, 2000. Vibrations of a taut cable with an external damper. Journal of Applied Mechanics, 67:772-776.
[8]   Main J A and Jones N P, 2002. Free vibrations of a taut cable with attached damper. I: Linear viscous damper, Journal of Engineering Mechanics, **128**:1062-1071.
[9]   Cu V H and Han B, 2015. A stay cable with viscous damper and tuned mass damper. Australian Journal of Structural Engineering, **16**:4, 316-323
[10]   Cai C S, Wu W J, Shi X M, 2006. Cable vibration. reduction with a hung-on TMD system. Part I: Theoretical study. Journal of Vibration and Control, **12**(7):801-814.
[11]   Smith M C, 2002 Synthesis of mechanical networks: The inerter. IEEE Transactions on Automatic Control, **47** (10): 1648.
[12]   Smith M C and Wang F C, 2004. Performance benefits in passive vehicle suspensions employing inerters. Vehicle System Dynamics, **42**(4), 235–257.
[13]   Evangelou S, Limebeer D J N, Sharp R S and Smith M C, 2004. Steering compensation for high-performance motorcycles. In Proceedings of the 43rd IEEE Conference on Decision and control, pp. 749–754.
[14]   Jiang J Z, Matamoros-Sanchez A Z, Goodall R M & Smith M C, 2012. Passive Suspensions Incorporating Inerters for Railway Vehicles. Vehicle System Dynamics, pp. 263-276
[15]   Jiang J Z, Matamoros-Sanchez A Z, Zolotas A, Goodall R M, & Smith M C, 2015. Passive suspensions for ride quality improvement of two-axle railway vehicles. Proceedings of the Institution of Mechanical Engineers, Part F: Journal of Rail and Rapid Transit, **229** (3). pp. 315-329.
[16]   Wang F, Su W, and Chen C, 2010. Building suspensions with inerters. Proceedings of the Institution of Mechanical Engineers, Part C, Journal of Mechanical Engineering Science 2010; **224**:1650–1616.
[17]   Lazar I F, Neild S A and Wagg D J, 2014. Using an inerter-based device for structural vibration suppression. Journal of Earthquake Engineering and Structural Dynamics, **43**(8):1129-1147.
[18]   Lazar I F, Neild S A and Wagg D J, 2015. Performance Analysis of Cables with Attached Tuned-Inerter-Dampers. Dynamics of Civil Structures, Volume **2**, pp 433-441
[19]   The MathWorks, Inc., MATLAB R2013a. Natick, Massachusetts, United States.